

Al₅O₄: A Superatom with Potential for New Materials Design

Ujjal Das and Krishnan Raghavachari*

Department of Chemistry, Indiana University, Bloomington, Indiana 47405

Received June 19, 2008

Abstract: The Al₅O₄[−] cluster displays a highly symmetric (D_{4h}) planar ring structure and magic cluster stability. The enhanced stability of this nonstoichiometric cluster is the result of an unconventional electronic distribution within the cluster, which is different from that found in stoichiometric Al₂O₃. The corresponding neutral Al₅O₄ cluster exhibits a strong electron affinity (3.5 eV) that is very close to that of a chlorine atom (3.6 eV). When interacting with the electropositive metals (M = Li, Na, K, etc.), the neutral cluster captures one electron and forms a “binary salt” composed of Al₅O₄[−] anion and M⁺ cation. Interestingly, the geometric and electronic structure of bare Al₅O₄[−] is completely retained in the salt structure. This suggests that Al₅O₄ behaves as a superatom and Al₅O₄M is reminiscent of a diatomic ionic molecule such as NaCl or KCl. We have also demonstrated that Al₅O₄M can be used as a building block to construct new solid state materials. A detailed structural analysis of the monomer, dimer, and trimer of Al₅O₄M reveals that while M tends to coordinate with the cluster oxygen in monomeric Al₅O₄M, the binding preference is significantly changed in the presence of multiple metal and cluster ions. In this case, M favors coordinating to the terminal Al atoms in the cluster where the four highest occupied molecular orbitals are distributed. Based on these observations, we have designed new 1-D, 2-D, and 3-D extended networks using Al₅O₄M as the building block. The 3-D periodic lattice displays a structure similar to that in zeolites and, therefore, may exhibit behavior useful for applications as molecular sieves.

Introduction

Clusters are ensembles of bound atoms intermediate in size between a molecule and the bulk solid. There are certain clusters with exceptionally high stability compared to their immediate neighbors. These are known as magic clusters. A few well-known examples of magic clusters are C₆₀,¹ Ti₈C₁₂,² Au₂₀,³ Al₁₃[−],⁴ the endohedral M@Au₁₂ cages,^{5–7} the aromatic B₁₂ cluster,⁸ and the polyhedral (V₂O₅)_n cages.^{9,10} Their high stability is typically characterized by high symmetry in the structure, saturated electronic shell, chemical inertness, and a large energy separation between the highest occupied and the lowest unoccupied molecular orbitals. In recent years, the quest to assemble these stable individual cluster units into new solid state materials has gathered a lot of momentum.^{11–19} One big advantage in this approach is the opportunity to tune the electronic and magnetic

properties of the new materials based on the user choice.¹⁸ However, there are many practical difficulties associated with this process. First of all, the clusters must retain their structural integrity in the assembled unit. Failure to do so often leads the cluster units to form oligomers. This is nicely documented in the all-metal aromatic cluster, M_n(Al₄^{2−}), where M represents an alkali or alkaline earth metal.²⁰ When brought together, two such units initiate interatomic bonding within the clusters rather than being stabilized into two separate units held together by electrostatic interactions. There may be other significant factors to be considered in such cluster-assembled materials related to the size of the clusters, heat of the lattice formation, etc. For example, Castleman and co-workers have shown that the size of the Al₁₃ superatom⁴ is too big to fit with counterions such as the alkali metals. They have recently proposed new super-alkali motifs (Na₃O and K₃O) to overcome this size mismatch.¹⁶ Nevertheless, the cluster-based approach to design

* Corresponding author e-mail: kraghava@indiana.edu.

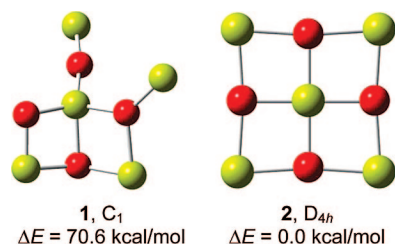


Figure 1. Lowest energy structure of Al_5O_4 (**1**) and Al_5O_4^- (**2**). Also shown are their symmetry and relative stability.

new nanomaterials with desired properties continues to be very fascinating. Herein, we report an aluminum oxide cluster anion, Al_5O_4^- , which shows magic cluster stability, and the corresponding neutral behaves like a superatom. Using first principles electronic structure calculations, we have shown that this metal oxide cluster can be assembled into different extended systems having diverse geometric and electronic properties. Given that the predicted 3D systems show zeolite-shaped structures, such materials, if synthesized, might find useful applications as molecular sieves.

Computational Methods

The geometry optimizations of the title species and other discrete molecular systems reported in this paper are performed using density functional theory (DFT). The B3LYP hybrid exchange-correlation functional, in conjunction with the multiply polarized 6-311+G(3df) basis set (valence triple- ζ 6-311G + three d -type and one f -type polarization functions + diffuse sp -functions) is used in the calculations.^{21–23} Geometry optimizations of extended systems, in 1D and 2D, are performed imposing periodic boundary conditions (PBC).^{24,25} Since PBC calculations using the hybrid DFT functionals such as B3LYP are prohibitively expensive, we use the PW91 functional with a moderate sized basis set, 6-311G(d). All these calculations are performed using the development version of the Gaussian quantum chemistry software package.²⁶

Geometry optimizations on the 3D extended systems have been performed using the DFT-based Vienna *ab initio* simulation package (VASP).^{27–30} The Perdew–Wang (PW91) exchange-correlation functional within the generalized gradient approximation (GGA) has been applied here.^{31–33} The calculations use ultrasoft pseudopotentials³⁴ and a plane wave basis set with an energy cutoff of 400 eV. The Brillouin zone is sampled using a $11 \times 11 \times 11$ k-point grid under the Monkhorst-Pack scheme.³⁵ The energy convergence criteria during geometry relaxation is set to 10^{-7} eV per atom. The geometries are well converged with respect to the plane-wave energy cutoff and k-point sampling. At the optimized geometry, the forces are converged to better than 0.6 meV/Å.

Results and Discussion

The Al_5O_4^- cluster was easily identified as a high intensity peak at 199 amu in the experimental mass spectra.³⁶ The lowest energy isomers of neutral (**1**) and anionic (**2**) forms of Al_5O_4 are shown in Figure 1. The neutral cluster possesses

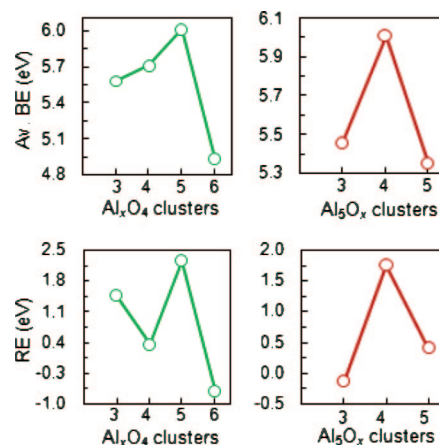


Figure 2. The top two boxes show the average atomic binding energy (see text) in Al_xO_4^- ($x = 3-6$) and Al_5O_x^- ($x = 3-5$) cluster series, respectively. The bottom two boxes show the local stability of each cluster with respect to the disproportionation schemes shown in eqs 3 and 4, respectively.

39 valence electrons. Interestingly, addition of one more electron to the neutral species produces a highly symmetric structure with alternating Al, O atoms along the periphery and an Al atom at the center of the ring (**2**). The central $\text{Al}_c\text{-O}$ bonds (1.78 Å) in **2** are in general shorter than the terminal $\text{Al}_t\text{-O}$ bonds (1.90 Å). It should be pointed out that though a B3LYP/6-31+G(d) calculation suggests a perfect square planar (D_{4h}) structure for the cluster anion, use of a larger basis set such as 6-311+G(3df) makes it slightly nonplanar. In this case, the five Al atoms are still in a plane, but the position of pairs of trans-oxygen atoms above and below this plane introduces a slight puckering and reduces the overall symmetry to D_{2d} . However, the deviation from planarity does not bring any notable changes in the structural parameters. Moreover, the energy difference between the planar D_{4h} structure and the slightly puckered D_{2d} structure is less than 1 kcal/mol. When zero-point energy corrections and finite temperature effects are considered, the difference in energy becomes even less. Hence we conclude that the vibrationally averaged structure of Al_5O_4^- is planar.³⁷

The relative stability of Al_5O_4^- with respect to its neighboring clusters can be estimated from the binding energies (BE) of their constituent atoms. The binding energy (BE) of aluminum in Al_xO_y^- is defined as the difference between the electronic energy of Al_xO_y^- and that of $\text{Al}_{x-1}\text{O}_y^- + \text{Al}$ (eq 1). The binding energy of oxygen is also defined in a similar way (eq 2).

$$BE(\text{Al}) = E(\text{Al}_x\text{O}_y^-) - E(\text{Al}_{x-1}\text{O}_y^-) - E(\text{Al}) \quad (1)$$

$$BE(\text{O}) = E(\text{Al}_x\text{O}_y^-) - E(\text{Al}_x\text{O}_{y-1}^-) - E(\text{O}) \quad (2)$$

The average binding energy per atom (i.e., the average of the Al and O binding energies as defined above) in two different cluster series (Al_xO_4^- and Al_5O_x^-) is shown in the top two boxes in Figure 2. In the first case (top-left), the number of metal atoms has been altered, while in the second case (top-right), the number of oxygen atoms has been changed. In both cases, a sharp peak at Al_5O_4^- suggests that

the fragmentation of the heavier species may end up enhancing the population of Al₅O₄[−]. Also note that the average binding energy in Al₅O₄[−] is approximately 6 eV per atom. This is comparable to the binding energy of atoms in other stable clusters such as fullerenes (e.g., C₆₀) and metacars (e.g., Ti₈C₁₂).³⁸

As an alternative way to measure the stability of the clusters, we can consider two disproportionation schemes shown in eqs 3 and 4.



The relative stability of the species on the left-hand side of the equation compared to the species on the right-hand side gives a good estimation of the local stability of the individual cluster. They are presented in the lower panels of Figure 2. Once again a sharp peak at Al₅O₄[−] indicates a strong resistance toward changes in the current composition. All these observations justify the magic cluster stability of Al₅O₄[−].

The chemical bond analysis in Al₅O₄[−] reveals why this cluster is so much more stable. While in stoichiometric Al₂O₃, both Al and O are in their formal oxidation states (Al³⁺ and O^{2−}), the electronic distributions in the nonstoichiometric aluminum oxide clusters are different. The central Al atom in Al₅O₄[−] contributes three electrons toward bonding, while the remaining four metal atoms donate one electron each. This leaves a total of eight electrons (3+4+1) in the anionic cluster which are then equally shared by four oxygen atoms. All the atoms in the cluster now have saturated electronic shells (3s² for the four terminal aluminum atoms and 2p⁶ for the central aluminum and the four oxide ions), and the resulting strong ionic bonding contributes toward the enhanced stability of the cluster. Such a bonding scenario also explains the large structural change in going from the neutral to the anionic cluster and suggests that neutral Al₅O₄ should have a strong electron affinity.

The adiabatic electron binding energy in Al₅O₄[−], which is equivalent to the adiabatic electron affinity (EA) of neutral Al₅O₄, is computed to be 3.46 eV. The corresponding vertical electron detachment energy is computed to be 3.75 eV. These two energies reconcile well with the experimental negative ion photoelectron spectra of Al₅O₄[−] where the first peak appears at around 3.8 eV with a tail at 3.5 eV.^{36,39} The difference of 0.3 eV between these two energies is significant and, in fact, supports our previous observation that there is a considerable geometric change between the neutral and the anion cluster. Note that the EA of Al₅O₄ is very close to that of the chlorine atom (3.6 eV), the element with the highest EA in the periodic table. The very strong electron binding energy, high symmetry, and high stability of the anionic cluster motivate us to verify if Al₅O₄ behaves as a superatom.

To verify this, we have considered the neutral “salt” Al₅O₄K. The geometries of its two lowest energy isomers are shown in Figure 3.⁴⁰ The only difference between **3** and **4** is the relative position of K. While K occupies a position facing an O atom in **3**, it occupies a position opposite a

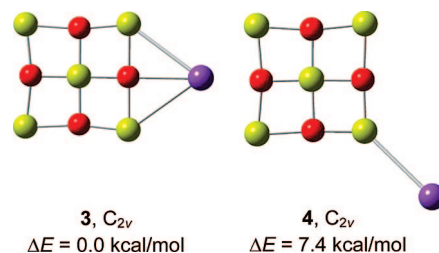


Figure 3. The two lowest energy isomers of Al₅O₄K and their relative stability.

Table 1. Selected Bond Lengths, Bond Angles, and NBO Atomic Charges of Al₅O₄[−] and Two Isomers of Al₅O₄K

parameters	Al ₅ O ₄ [−]	Al ₅ O ₄ K (3)	Al ₅ O ₄ K (4)
Bond Lengths (Å)			
Al _c –O	1.785	1.813/1.787	1.808/1.767
Al _t –O	1.902	1.817/1.905	1.813/1.939
Bond Angles (°)			
O–Al _t –O	83.1	84.2/81.1	87.6/81.7
NBO Charges (e)			
O	−1.57	−1.59	−1.57
Al _c	2.08	2.11	2.09
Al _t	0.80	0.87	0.84
K	NA	0.77	0.82

terminal Al atom in **4**. **3** is energetically more stable than **4**. The binding energies of K in **3** and **4** are −48 and −41 kcal/mol, respectively. The distance between K and O in **3** is 2.66 Å, which is nearly 0.7 Å shorter than the distance between K and Al in **4**. However, we will see later that this binding preference is actually reversed when the cluster is surrounded by multiple metal atoms. As expected, the presence of K atom in Al₅O₄K reduces the high symmetry observed in bare Al₅O₄[−]. This is reflected in the corresponding structural parameters shown in Table 1. However, it is surprising that the net changes in the bond lengths and bond angles between Al₅O₄[−] and Al₅O₄K are not very significant. For example, the maximum deviations in Al_c–O and Al_t–O distances and in the O–Al_t–O angle between these two species are 0.03 Å, 0.09 Å, and 4.5°, respectively. The maximum deviations are observed in the vicinity of K. As the distance of the cluster atoms from K increases, these differences become even smaller. Moreover, NBO population analysis shows that the charge on K atom in Al₅O₄K is +0.8e, clearly suggesting that the alkali atom loses one electron on bond formation. A careful analysis reveals that there are almost no changes in the individual atomic charges when comparisons are made between bare Al₅O₄[−] and the Al₅O₄ segment in Al₅O₄K. This indicates that the electron lost by K is mostly captured by the cluster moiety and that the compound Al₅O₄K is actually a “binary salt” consisting of K⁺ and Al₅O₄[−] ions. All these observations suggest that the electronic and structural integrity of Al₅O₄[−] are retained even when it interacts with the metal atoms.

A third isomer of Al₅O₄K where K interacts with the central Al atom of the cluster from the top has also been considered. The optimized structure is shaped like an “umbrella” (C_{4v} symmetry) and is considerably less stable than the two other isomers (**3** and **4**). The lower stability in

this isomer is perhaps due to the unfavorable interaction between the electron deficient central aluminum atom and the K^+ ion.

The metal-halide salts are generally characterized by very large dipole moments. For example, the dipole moments of NaCl and KCl in the gas phase are 9 and 10 D, respectively.^{41,42} The dipole moment of the potassium salt of $Al_5O_4^-$ anion is 11 D.^{43,44} Similarly, we have computed a very large dipole moment in Al_5O_4K (13 D in **3** and 19 D in **4**). The orientations of the dipole vectors in these molecules, from the center of the cluster anion toward the cation, resemble the directions of dipole vectors in model compounds such as NaCl or KCl. This is again strongly indicative that Al_5O_4K indeed behaves as a diatomic ionic molecule.

The large energy difference between the highest occupied (HOMO) and the lowest unoccupied (LUMO) molecular orbital is a good measure of the chemical inertness of a species. For example, the HOMO–LUMO energy gap in Al_5O_4K , which also behaves like a stable diatomic ionic molecule as shown by Bowen and co-workers, is observed to be 1.3 eV.³⁸ As_7K_3 is another stable cluster where this gap is measured to be 2.2 eV by Castleman et al.¹⁵ Using TDDFT calculations, we have computed the energy required to excite an electron from the doubly filled HOMO of Al_5O_4K to the LUMO without allowing any geometric changes. This gives an estimation of the HOMO–LUMO gap in the system, which is found to be 1.6 eV. The relatively large energy gap indicates that Al_5O_4K is also chemically inert and especially suitable to serve as a building block for designing new materials. However, note that the structure and the HOMO–LUMO energy gap of Al_5O_4K described here are purely computational. This and the remaining gas phase molecules reported in this study are subject to the experimental verifications.

The integrity of Al_5O_4K structure has also been verified by exchanging the positions of terminal Al and K atoms in **3** and **4**. The K atom is now a part of the cluster unit. Since we already know from population analysis that formal charges on both of these atoms are close to +1, this alternation does not perturb the electronic distribution of the system. During geometry optimization one of these structures rearranges back into **3**, while the other optimized structure appears to be far less stable than either **3** or **4**. This confirms yet again that **3** is most stable among all these isomers.

Next we try to incorporate the individual cluster unit into real 1-D, 2-D, and 3-D networks. For this, we need to understand the orientation of the counterions around $Al_5O_4^-$ and vice versa. First we consider the species, $Al_5O_4K_4$, and set the overall charge to +3 to make sure that it corresponds to the $Al_5O_4^-$ ion surrounded by four K^+ ions. **5** and **6** in Figure 4 show the positions of the K^+ ions around an $Al_5O_4^-$ unit. **6** is about 36 kcal/mol more stable than **5**. In fact, **5** is not a minimum and has an imaginary vibrational mode that leads to **6**. This clearly suggests that the corner positions are preferred over the center of each side of the cluster when multiple potassium ions are present. A similar tendency was previously observed by Hoffmann and co-workers where they found that Li^+ ions bind more strongly at the four corners of the planar tetracoordinate carbon unit, C_5^{2-} .¹⁴ This trend

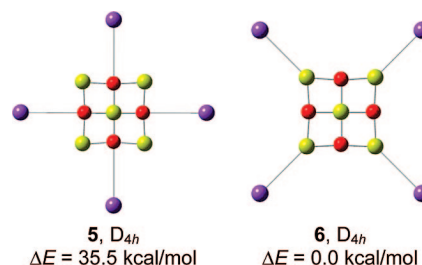


Figure 4. Two possible isomers of $Al_5O_4K_4^{3+}$ showing the preferred orientation of the cations around the cluster anion.

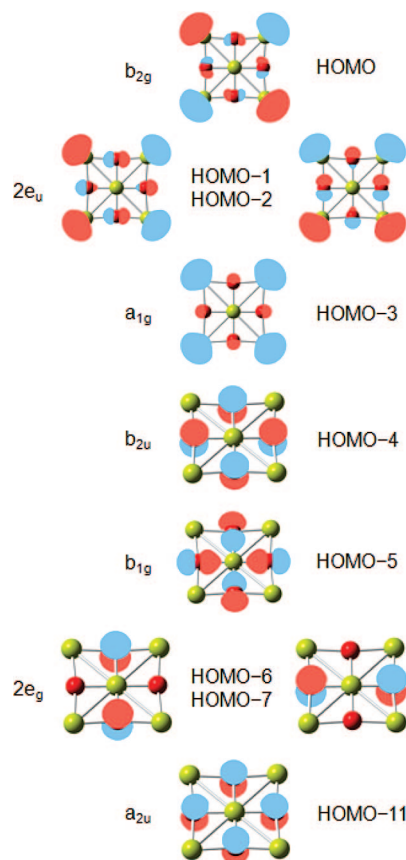


Figure 5. Molecular orbital (MO) energy diagram of $Al_5O_4^-$ showing selected orbitals. Note that the four highest occupied orbitals represent lone pairs on terminal Al atoms.

appears to be different from our earlier observation that isomer **3** is more stable than **4**. However, the higher stability of **6** relative to **5** can be understood from a careful analysis of the interactions between the species. Figure 5 displays the high-lying molecular orbitals of $Al_5O_4^-$ in their respective energy order. Note that the lone pair electrons on the terminal Al atoms in $Al_5O_4^-$ are distributed among the four highest occupied molecular orbitals. In contrast, the orbitals associated with the electron pairs on the oxygen atoms appear lower down the energy scale. As a result, the strong electrophilic interactions between K^+ ions and the lone pairs on the terminal Al atoms explain the higher stability of **6**.

The preference for metal–Al coordination over metal–O coordination can also be understood from the position of the Dyson orbitals in $Al_5O_4^-$. As shown by Guevara-Garcia et al., the Dyson orbitals of three final states after detaching

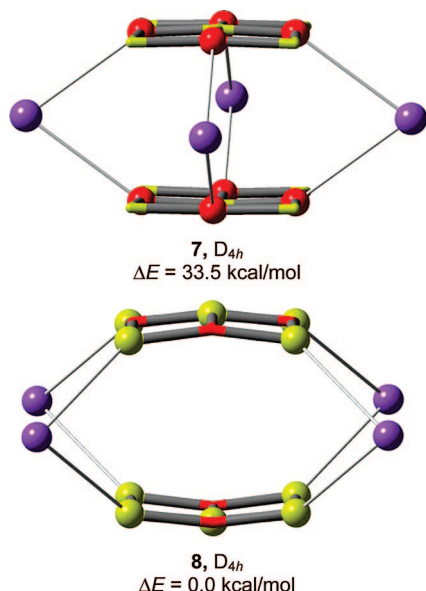


Figure 6. Two possible isomers of $(\text{Al}_5\text{O}_4)_2\text{K}_4^{2+}$ showing the preferred nonplanar orientation of the clusters.

an electron from this cluster consist chiefly of Al (terminal) 3s functions with minor antibonding oxygen contributions.⁴⁵ This suggests that in the interaction of neutral Al_5O_4 with K, the electron released by the metal will be mostly captured by the terminal aluminums. Also note that the absence of Dyson orbital amplitude at the central Al makes it the most preferred position for a nucleophilic attack. This is in fact observed in the reaction of Al_5O_4^- with the nucleophiles such as water, ammonia, and methanol.^{36,45,46}

Next, we consider different structural isomers of $(\text{Al}_5\text{O}_4)_2\text{K}_4^{2+}$ in order to understand the possible nonplanar arrangements of the cluster assemblies. We begin with **7** where the two cluster units are stacked on top of each other and the four K atoms are positioned in a separate layer in between the planes of the clusters. This is somewhat analogous to the structure of sandwich complexes such as ferrocene. As shown in Figure 6, the metal atoms in this configuration are actually facing the oxygen atoms in the cluster. However, we have found that **7** is a first order saddle point on the potential energy surface. When the displacement vectors of the corresponding imaginary frequency are followed, the optimization leads to structure **8**. **8** is 34 kcal/mol more stable than **7**. In **8**, the metal ions are facing the corner Al atoms, consistent with the previously observed trend.

As we have mentioned briefly in the Introduction, it is possible sometimes that the structural integrity of the individual cluster may collapse when two such units interact with each other. This is usually due to the formation of intercluster atomic bonds, which initiates the collapse. If so, then predicting an extended system using such clusters as building blocks has to be regarded with some caution. We want to verify this point for the $\text{Al}_5\text{O}_4\text{K}$ unit. In particular, we want to see if Al–Al bond formation leading to a thermodynamically more stable product is feasible. Since each terminal aluminum atom contains one nonbonding electron pair, it is unlikely that the interaction between two terminal atoms will stabilize the system to any significant

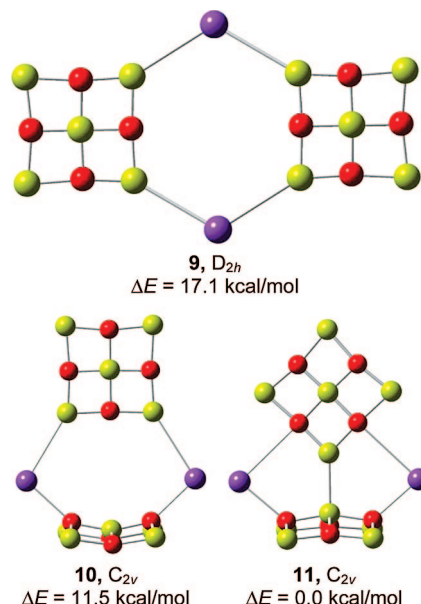


Figure 7. Three different isomers of $(\text{Al}_5\text{O}_4\text{K})_2$ dimer and their relative stability.

extent. However, since the central aluminum is electron deficient, it can induce an ion-dipole type interaction with a polar end of another cluster, which may result in some bonding interaction between the two clusters.

To gain insight into how two $\text{Al}_5\text{O}_4\text{K}$ units interact with each other, we have considered many different structures and found dimers **9–11** as the three lowest energy isomers (Figure 7). Note the relative positions of the cations in these isomers. **9** is planar and the K atoms are only pointed toward the terminal aluminums. **10** shows a nonplanar arrangement of the clusters where the alkali metals are facing both Al and O atoms. **11** shows a different nonplanar arrangement of the clusters where the K atoms are only facing the cluster oxygen atoms. Additional ion-dipolar interaction between the central (in +3 state) and terminal (contains lone pair) aluminums is also found in **11**, which makes it the most stable among all three dimers. As a result of this interaction, the central metal atom slightly projects out of the cluster surface. The $\text{Al}_c\text{--Al}_t$ distance is 2.61 Å. Nonetheless, the structural integrity of the two clusters in **11** is mostly retained. We will see next which of these three structural patterns is actually translated in an extended system.

Alternative isomers considering the interactions between the oxygens of one cluster and the aluminums of another cluster also have been generated. Their optimized geometries are comparatively less stable than the ones described above. This suggests that the dimerization via formation of Al–Al bonds is energetically more preferable than Al–O bond formation.

We have already observed that in the presence of multiple cations, the $\text{Al}_t\text{--K}$ interactions are energetically favored over O–K interactions for both planar and nonplanar arrangement of the counterions (isomers **6** and **8**). This gives a first order approximation that in an extended system the structural pattern found in **9** should get preference over the other dimers. This has been further verified here. Shown in Figure 8 are the optimized structures of three trimers designed based

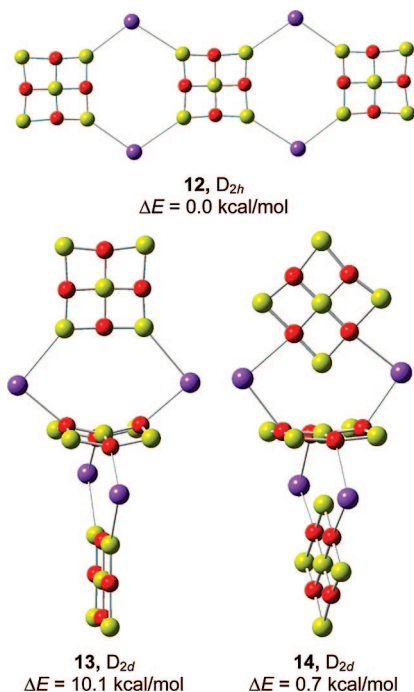


Figure 8. Three different isomers of $(\text{Al}_5\text{O}_4\text{K})_3$ trimer and their relative stability. One additional K^+ ion in the trimer structure has been added to maintain the structural building blocks.

on the corresponding dimer structures. One additional K is placed to maintain the structural building blocks (leading to a high symmetry), and the overall charge is set to +1 to retain the proper electronic distribution. Note the stability order of these three isomers. The large energy difference observed in case of the dimers favoring the nonplanar configurations does no longer exist. Instead the planar configuration **12** is now energetically competitive with **14** and, in fact, slightly more stable. This indicates that the ion-dipolar interactions are not as dominant as the number of clusters in the oligomer increases. These results strongly suggest that the structural pattern found in **4**, **9**, and **12** will lead to a stable extended system.

Optimized structures of the extended 1-D and 2-D networks are displayed in Figure 9. **15** is obtained by expanding structure **4** in one dimension. On the other hand, **16** repeats the trend observed in **9** and **12** in two dimensions. **16** belongs to the $P4mm$ space group. The length of the unit cell vectors in these two systems is given in Table 2. In each unit cell, there is exactly one cluster anion and one K^+ ion, thus maintaining the overall charge neutrality. The $\text{Al}_i\text{--K}$ distances are slightly elongated than the values observed in the discrete molecular systems. However, the Al--O distances do not show any significant changes. To examine how the HOMO–LUMO energy gaps of the cluster motifs evolve as they are brought together to form the solid, a comparison is made in Figure 10. Note that the HOMO–LUMO gap of 1.6 eV in $\text{Al}_5\text{O}_4\text{K}$ increases significantly to 3.2 eV in the corresponding dimer. This is because when two $\text{Al}_5\text{O}_4\text{K}$ units interact with each other, the corresponding HOMOs are stabilized while the LUMOs are destabilized, increasing the overall energy gap. However, the gap in the trimer unit is reduced to 2.3 eV due to orbital interactions of the additional cluster. Interestingly, a similar band gap is computed for the

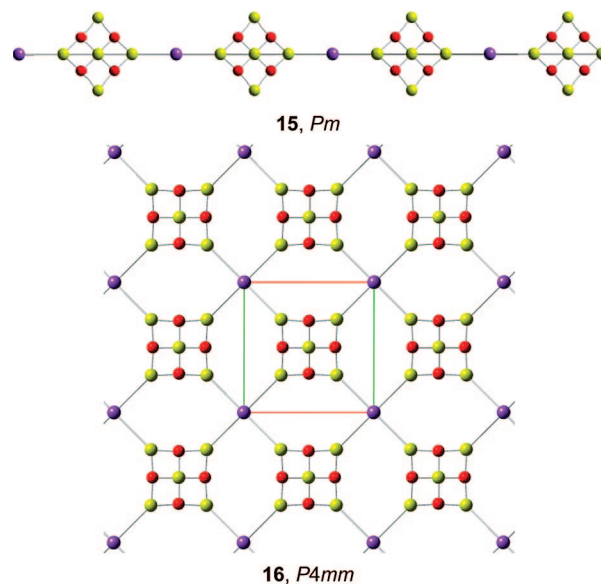


Figure 9. Optimized 1-D and 2-D networks using $\text{Al}_5\text{O}_4\text{K}$ as building blocks.

Table 2. Space Group, Unit Cell Parameters (\AA), z Value, and Volume (\AA^3) of Different Extended Networks

system	space group	z	a	b	c	V
15	Pm	1	12.23			
16	$P4mm$	1	8.90	8.90		
17	$P\bar{4}m2$	1	7.15	7.15	13.26	677.35
18	$P4/mmm$	1	8.17	8.17	3.11	207.95

extended networks **15** and **16**. This shows that the electronic properties of the cluster motifs are more or less retained in the extended structures.

Based on the above observations, we have designed a 3-D network displayed in Figure 11. **17** belongs to the $P\bar{4}m2$ space group, and the crystal has a tetragonal unit cell. An extended view of the crystal structure is also presented in Figure 11. Note that the local coordination of the cation in **17** is tetrahedral. Since K is less known for this type of coordination, we have used copper(I) as the counterion. Cu(I) compounds such as chlorides and oxides are known to exhibit a similar coordination for the metal center. In each unit cell, there are two Al_5O_4^- and two Cu(I) atoms. The Cu–Al distance is 2.24 \AA , approximately 0.3 \AA shorter than the sum

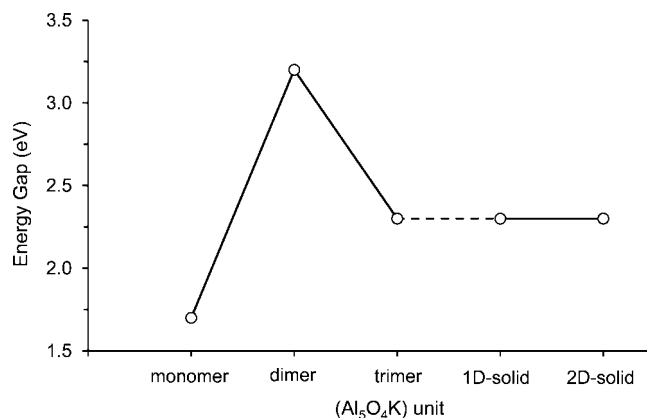


Figure 10. Variation in energy gap (HOMO–LUMO gap for clusters and band gap for solids).

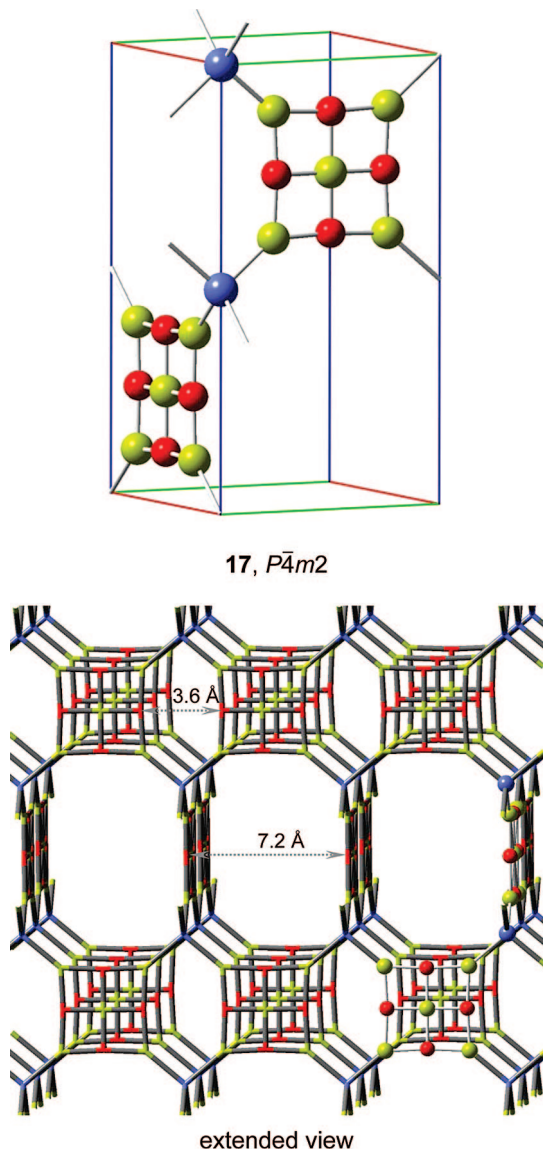
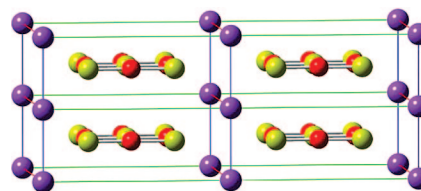


Figure 11. Unit cell (top) and an extended view (bottom) of a 3-D network of Al₅O₄Cu.

of their atomic radii. This confirms the ionic type of interaction between the species. The average computed lengths for Al_c–O and Al_t–O bonds are 1.78 Å and 1.87 Å, respectively. These values can be compared to the corresponding lengths of 1.78 Å and 1.90 Å in the bare cluster, which suggests very little structural change in the extended system. The angles around the Cu atom deviate somewhat from the ideal tetrahedral value of 109.5°. The Al_t–Cu–Al_t angles along the unit cell axes are in general shorter (99.7°) than the same angles between two different axes (114.6°).

The effective diameter of the larger pores in **17** is 0.72 nm (7.2 Å), while the diameter of the smaller pores is about half of this size (0.36 nm). The molecular diameter of H₂ ($\sigma_{\text{eff}} = 0.30$ nm) and N₂ ($\sigma_{\text{eff}} = 0.36$ nm) are comparable to the size of the small pores. On the other hand, hydrocarbon molecules such as propane, butane, and pentane are suitable to fit into the large pores. Therefore, the polar interior of the three-dimensional lattice may be selectively able to bind inorganic and organic molecules in these pores. This opens



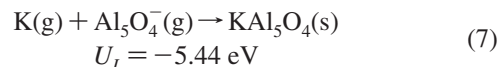
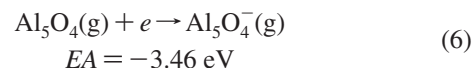
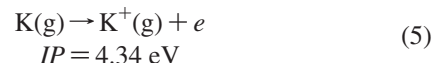
18, $P4/mmm$

Figure 12. Unit cell of a 3-D network of Al₅O₄K.

up the possibility that these zeolite-shaped structures can find important applications as storage materials and molecular sieves.

An alternative 3-D network, **18**, has been constructed based on structure **8**. **18** belongs to the $P4/mmm$ space group, and the unit cell represents a body-centered tetragonal lattice (Figure 12). The alkali metals are placed at eight corners of the tetragonal lattice, while the anion occupies the body-center position. Thus each unit cell maintains a 1:1 ratio of the counterions. The unit cell parameters are presented in Table 2. The Al_t–K (3.49 Å), Al_c–O (1.79 Å), and Al_t–O (1.88 Å) distances do not change much from the discrete molecular systems. The K–Al_t–K angles are 53°.

Given that the ionization potential (IP) of K (4.34 eV) is higher than the electron affinity (EA) of Al₅O₄ (3.46 eV), the formation of K⁺ and Al₅O₄[−] from individual molecules is slightly endothermic. However, the substantial Madelung energy resulting from the ionic lattice is expected to make the Al₅O₄K lattice formation to be highly exothermic. The lattice energy (U_L) can be estimated using the Kapustinskii equation (eq 8).⁴⁷ In this equation, ν is the number of ions in the empirical formula, z is the anionic and cationic charge, respectively, and r is the radius of the anion (2.69 Å) or cation (1.51 Å). It is important to remember that the unit of the lattice energy in this equation is given in kJ/mol, which is finally converted into electronvolt (eV). As shown in eq 9, overall the Al₅O₄K lattice formation is a thermodynamically favorable process.



$$U_L = -1202 \times \frac{\nu |z^+| \cdot |z^-|}{y^+ + y^-} \times \left(1 - \frac{0.345}{y^+ + y^-} \right) \quad (8)$$

$$\Delta H = IP + EA + U_L = -4.56 \text{ eV} \quad (9)$$

Finally, we would like to add some comments on the reactivity of Al₅O₄K. In particular, it is preferable for such predicted extended systems to be chemically stable especially in the presence of common solvent systems such as water. We have previously seen that small polar molecules such as water or methanol dissociatively add to the center of Al₅O₄[−].^{36,46} Although surprisingly, ammonia, being a similar type of molecule, does not react. Since Al₅O₄[−] and Al₅O₄K have similar electronic structures, the latter may also show

similar chemical reactivity with the above molecules. However, this might not be the case for the extended systems. In the case of the monomer reactions, all these reactions are induced by initial charge-dipole type interactions between a lone pair on water and the central aluminum of the cluster anion. We have shown earlier in this paper that such charge-dipolar interaction becomes less dominant when the individual cluster units start to agglomerate. In addition, the less open access to the central aluminum due to the presence of the counterions may also lead to a less reactive environment. This gives some indication that the extended lattice may show chemical resistance against water or methanol. However, we note that, though preferable, such chemical inertness is not a requirement for the viability of formation of such materials.

Conclusions

In summary, we have shown that the aluminum oxide cluster anion Al_5O_4^- exhibits a highly symmetric planar structure and magic cluster stability. The electron affinity of neutral Al_5O_4 is similar to that of chlorine, the element with the largest electron affinity in the periodic table. When interacting with electropositive metals such as Na and K, the neutral Al_5O_4 extracts an electron from the metal to form a binary salt $\text{Al}_5\text{O}_4\text{M}$ consisting of Al_5O_4^- and M^+ ions. The electronic and structural integrity of bare Al_5O_4^- is completely retained in the salt structure. After a detailed structural analysis of dimers and trimers of the $\text{Al}_5\text{O}_4\text{M}$ unit, we have designed different extended periodic networks using $\text{Al}_5\text{O}_4\text{M}$ as building blocks. The predicted 3-D networks exhibit zeolite-shaped structure and contain pores of different diameters. This opens up the possibility that such new nanomaterials, if synthesized, may find potential application as molecular sieves.

Acknowledgment. We gratefully acknowledge funding from the National Science Foundation (NSF grant CHE-0616737).

Supporting Information Available: Coordinates of the discrete molecules and periodic systems. This material is available free of charge via the Internet at <http://pubs.acs.org>.

References

- (1) Kroto, H. W.; Heath, J. R.; O'Brien, S. C.; Curl, R. F.; Smalley, R. E. *Nature* **1985**, *318*, 162.
- (2) Guo, B. C.; Kerns, K. P.; Castleman, A. W. *Science* **1992**, *255*, 1411.
- (3) Li, J.; Li, X.; Zhai, H. J.; Wang, L. S. *Science* **2003**, *299*, 864.
- (4) Bergeron, D. E.; Castleman, A. W.; Morisato, T.; Khanna, S. N. *Science* **2004**, *304*, 84.
- (5) Li, X.; Kiran, B.; Li, J.; Zhai, H. J.; Wang, L. S. *Angew. Chem., Int. Ed.* **2002**, *41*, 4786.
- (6) Pyykko, P.; Runeberg, N. *Angew. Chem., Int. Ed.* **2002**, *41*, 2174.
- (7) Zhai, H. J.; Li, J.; Wang, L. S. *J. Chem. Phys.* **2004**, *121*, 8369.
- (8) Zhai, H. J.; Kiran, B.; Li, J.; Wang, L. S. *Nat. Mater.* **2003**, *2*, 827.
- (9) Asmis, K. R.; Santambrogio, G.; Brummer, M.; Sauer, J. *Angew. Chem., Int. Ed.* **2005**, *44*, 3122.
- (10) Zhai, H. J.; Dobler, J.; Sauer, J.; Wang, L. S. *J. Am. Chem. Soc.* **2007**, *129*, 13270.
- (11) Khanna, S. N.; Jena, P. *Phys. Rev. B* **1995**, *51*, 13705.
- (12) Khanna, S. N.; Jena, P. *Phys. Rev. Lett.* **1992**, *69*, 1664.
- (13) Geske, G. D.; Boldyrev, A. I. *Inorg. Chem.* **2002**, *41*, 2795.
- (14) Pancharatna, P. D.; Mendez-Rojas, M. A.; Merino, G.; Vela, A.; Hoffmann, R. *J. Am. Chem. Soc.* **2004**, *126*, 15309.
- (15) Castleman, A. W.; Khanna, S. N.; Sen, A.; Reber, A. C.; Qian, M.; Davis, K. M.; Peppernick, S. J.; Ugrinov, A.; Merritt, M. D. *Nano Lett.* **2007**, *7*, 2734.
- (16) Reber, A. C.; Khanna, S. N.; Castleman, A. W. *J. Am. Chem. Soc.* **2007**, *129*, 10189.
- (17) Roach, P. J.; Reber, A. C.; Woodward, W. H.; Khanna, S. N.; Castleman, A. W. *Proc. Natl. Acad. Sci. U.S.A.* **2007**, *104*, 14565.
- (18) Yang, L. M.; Ding, Y. H.; Sun, C. C. *J. Am. Chem. Soc.* **2007**, *129*, 1900.
- (19) Yang, L. M.; Ding, Y. H.; Sun, C. C. *J. Am. Chem. Soc.* **2007**, *129*, 658.
- (20) Yang, L. M.; Ding, Y. H.; Sun, C. C. *Chem. Eur. J.* **2007**, *13*, 2546.
- (21) Krishnan, R.; Binkley, J. S.; Seeger, R.; Pople, J. A. *J. Chem. Phys.* **1980**, *72*, 650.
- (22) Lee, C. T.; Yang, W. T.; Parr, R. G. *Phys. Rev. B* **1988**, *37*, 785.
- (23) Becke, A. D. *J. Chem. Phys.* **1993**, *98*, 5648.
- (24) Kudin, K. N.; Scuseria, G. E. *Chem. Phys. Lett.* **1998**, *289*, 611.
- (25) Kudin, K. N.; Scuseria, G. E.; Schlegel, H. B. *J. Chem. Phys.* **2001**, *114*, 2919.
- (26) Frisch, M. J.; Trucks, G. W.; Schlegel, H. B.; Scuseria, G. E.; Robb, M. A.; Cheeseman, J. R.; Montgomery, J. A., Jr.; Vreven, T.; Scalmani, G.; Mennucci, B.; Barone, V.; Petersson, G. A.; Caricato, M.; Nakatsuji, H.; Hada, M.; Ehara, M.; Toyota, K.; Fukuda, R.; Hasegawa, J.; Ishida, M.; Nakajima, T.; Honda, Y.; Kitao, O.; Nakai, H.; Li, X.; Hratchian, H. P.; Peralta, J. E.; Izmaylov, A. F.; Kudin, K. N.; Heyd, J. J.; Brothers, E.; Staroverov, V. N.; Zheng, G.; Kobayashi, R.; Normand, J.; Sonnenberg, J. L.; Ogliaro, F.; Bearpark, M.; Parandekar, P. V.; Ferguson, G. A.; Mayhall, N. J.; Iyengar, S. S.; Tomasi, J.; Cossi, M.; Rega, N.; Burant, J. C.; Millam, J. M.; Klene, M.; Knox, J. E.; Cross, J. B.; Bakken, V.; Adamo, C.; Jaramillo, J.; Gomperts, R.; Stratmann, R. E.; Yazyev, O.; Austin, A. J.; Cammi, R.; Pomelli, C.; Ochterski, J. W.; Ayala, P. Y.; Morokuma, K.; Voth, G. A.; Salvador, P.; Dannenberg, J. J.; Zakrzewski, V. G.; Dapprich, S.; Daniels, A. D.; Strain, M. C.; Farkas, O.; Malick, D. K.; Rabuck, A. D.; Raghavachari, K.; Foresman, J. B.; Ortiz, J. V.; Cui, Q.; Baboul, A. G.; Clifford, S.; Cioslowski, J.; Stefanov, B. B.; Liu, G.; Liashenko, A.; Piskorz, P.; Komaromi, I.; Martin, R. L.; Fox, D. J.; Keith, T.; Al-Laham, M. A.; Peng, C. Y.; Nanayakkara, A.; Challacombe, M.; Chen, W.; Wong, M. W.; Pople, J. A. *Gaussian DV, revision G.01*; Gaussian Inc: Wallingford, CT, 2007.
- (27) Hohenberg, P.; Kohn, W. *Phys. Rev. B* **1964**, *136*, B864.
- (28) Kresse, G.; Hafner, J. *Phys. Rev. B* **1993**, *47*, 558.
- (29) Kresse, G.; Hafner, J. *Phys. Rev. B* **1994**, *49*, 14251.

- (30) Kresse, G.; Furthmüller, J. *Comput. Mater. Sci.* **1996**, 6, 15.
- (31) Perdew, J. P.; Yue, W. *Phys. Rev. B* **1986**, 33, 8800.
- (32) Perdew, J. P. In *Electronic Structure of Solids*; Ziesche, P., Eschrig, H., Eds.; Akademie Verlag: Berlin, Germany, 1991; p 11.
- (33) Payne, M. C.; Teter, M. P.; Allan, D. C.; Arias, T. A.; Joannopoulos, J. D. *Rev. Mod. Phys.* **1992**, 64, 1045.
- (34) Kresse, G.; Joubert, D. *Phys. Rev. B* **1999**, 59, 1758.
- (35) Monkhorst, H. J.; Pack, J. D. *Phys. Rev. B* **1976**, 13, 5188.
- (36) Das, U.; Raghavachari, K.; Jarrold, C. C. *J. Chem. Phys.* **2005**, 122, 014313.
- (37) Wang, L. S.; Boldyrev, A. I.; Li, X.; Simons, J. *J. Am. Chem. Soc.* **2000**, 122, 7681.
- (38) Zheng, W. J.; Thomas, O. C.; Lippa, T. P.; Xu, S. J.; Bowen, K. H. *J. Chem. Phys.* **2006**, 124, 144304.
- (39) Meloni, G.; Ferguson, M. J.; Neumark, D. M. *Phys. Chem. Chem. Phys.* **2003**, 5, 4073.
- (40) Many of the planar discrete molecular systems reported in this study contain imaginary frequency mode(s) that corresponds to a minor out-of-plane distortion of the cluster oxygens. See the text for a brief discussion of this mode for the parent cluster anion. The number of imaginary modes varies depending on the symmetry of the system. In most such cases, we have optimized a nonplanar structure taking into account the out-of-plane distortions that lead to lower energies. The energy difference between the planar and nonplanar configuration is always less than 1 kcal/mol. When zero-point energy corrections are considered, this energy difference is even smaller. This suggests that the vibrationally averaged structures of the reported molecules are planar, and, therefore, we have not discussed such imaginary modes in the text.
- (41) Clouser, P. L.; Gordy, W. *Phys. Rev. A* **1964**, 134, A863.
- (42) Leeuw, F. H. D.; Vanwache, R.; Dymanus, A. *J. Chem. Phys.* **1970**, 53, 981.
- (43) Ashman, C.; Khanna, S. N.; Pederson, M. R. *Phys. Rev. B* **2002**, 66, 193408.
- (44) Khanna, S. N.; Rao, B. K.; Jena, P. *Phys. Rev. B* **2002**, 65, 125105.
- (45) Guevara-Garcia, A.; Martinez, A.; Ortiz, J. V. *J. Chem. Phys.* **2007**, 127, 234302.
- (46) Das, U.; Raghavachari, K. *J. Chem. Phys.* **2007**, 127, 154310.
- (47) Huheey, J. E.; Keiter, E. A.; Keiter, R. L. In *Inorganic Chemistry: Principles of Structure and Reactivity*, 4th ed.; Pearson Education: Delhi, India, 2002; p 111.

CT800232B